Electronic Supplementary Material (ESI) for Dalton Transactions.
This journal is © The Royal Society of Chemistry 2018

Supplementary Information

Strong electronic influence of equatorial ligands on frontier orbitals in paddlewheel dichromium(II, II) complexes

Po-Jung Huang,[a] Yoshiki Natori,[b] Yasutaka Kitagawa,[b] Yoshihiro Sekine,[a,c] Wataru Kosaka,[a,c] and Hitoshi Miyasaka*[a,c]

[a] Department of Chemistry, Graduate School of Science, Tohoku University, 6-3 Aramaki-Aza-Aoba, Aoba-ku, Sendai 980-8578, Japan

[b] Department of Materials Engineering Science, Osaka University, 1-3 Machikaneyama-chou, Toyonaka, Osaka 560-0043, Japan

[c] Institute for Materials Research, Tohoku University, 2-1-1 Katahira, Aoba-ku, Sendai 980-8577, Japan

*Corresponding author:
Hitoshi Miyasaka
Institute for Materials Research, Tohoku University, 2-1-1 Katahira, Aoba-ku, Sendai 980-8577, Japan
Tel: +81-22-215-2030
Fax: +81-22-215-2031
E-mail: miyasaka@imr.tohoku.ac.jp

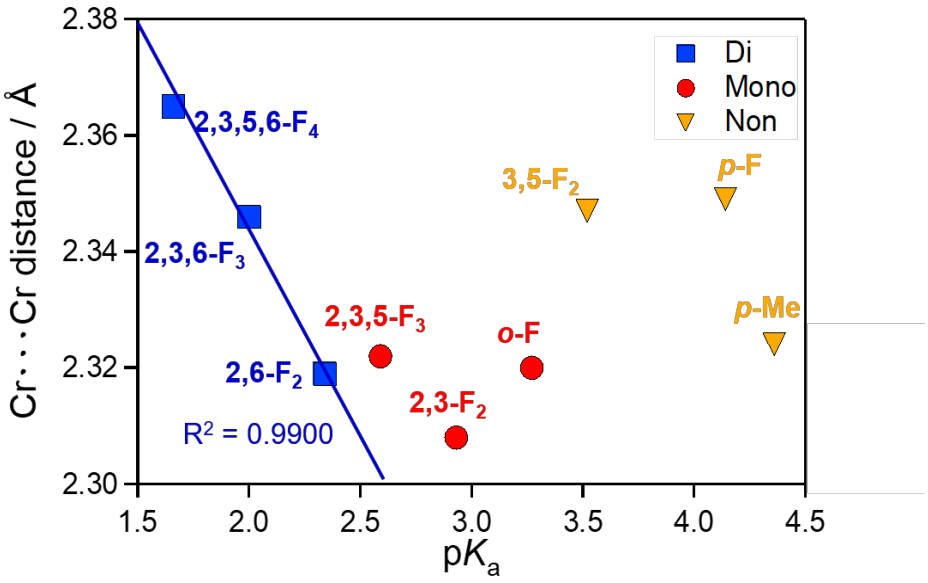

Figure S1. Plot of Cr···Cr distance vs. pK_a of corresponding benzoic acid with groups of di-*o*-F (blue filled square), mono-*o*-F (red filled circle), non-*o*-F (yellow filled triangle) representing compounds possessing respectively two, one, and no *ortho*-positioned fluorine substitution(s) on benzoate bridges, while the blue solid line represents the lease-squares linear fit for the di-*o*-F group.

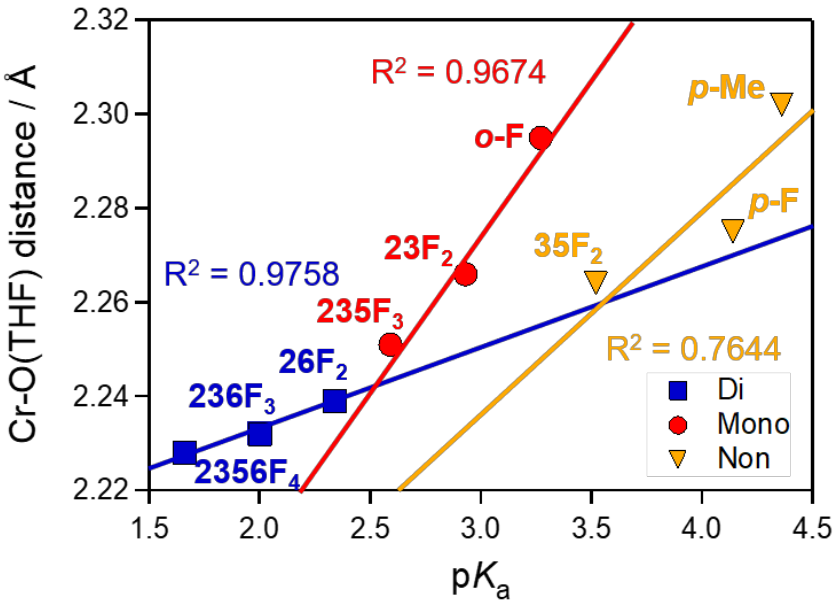

Figure S2. Plot of Cr−O_{THF} distance vs. pK_a for the series of [Cr_2] complexes with the same classification indicated in the caption of Fig. S1 with least square linear fits shown in solid lines. Strong correlation without regarding intermolecular interactions should be addressed by the negligible influence on Cr−O_{THF} part by π-π stacking.

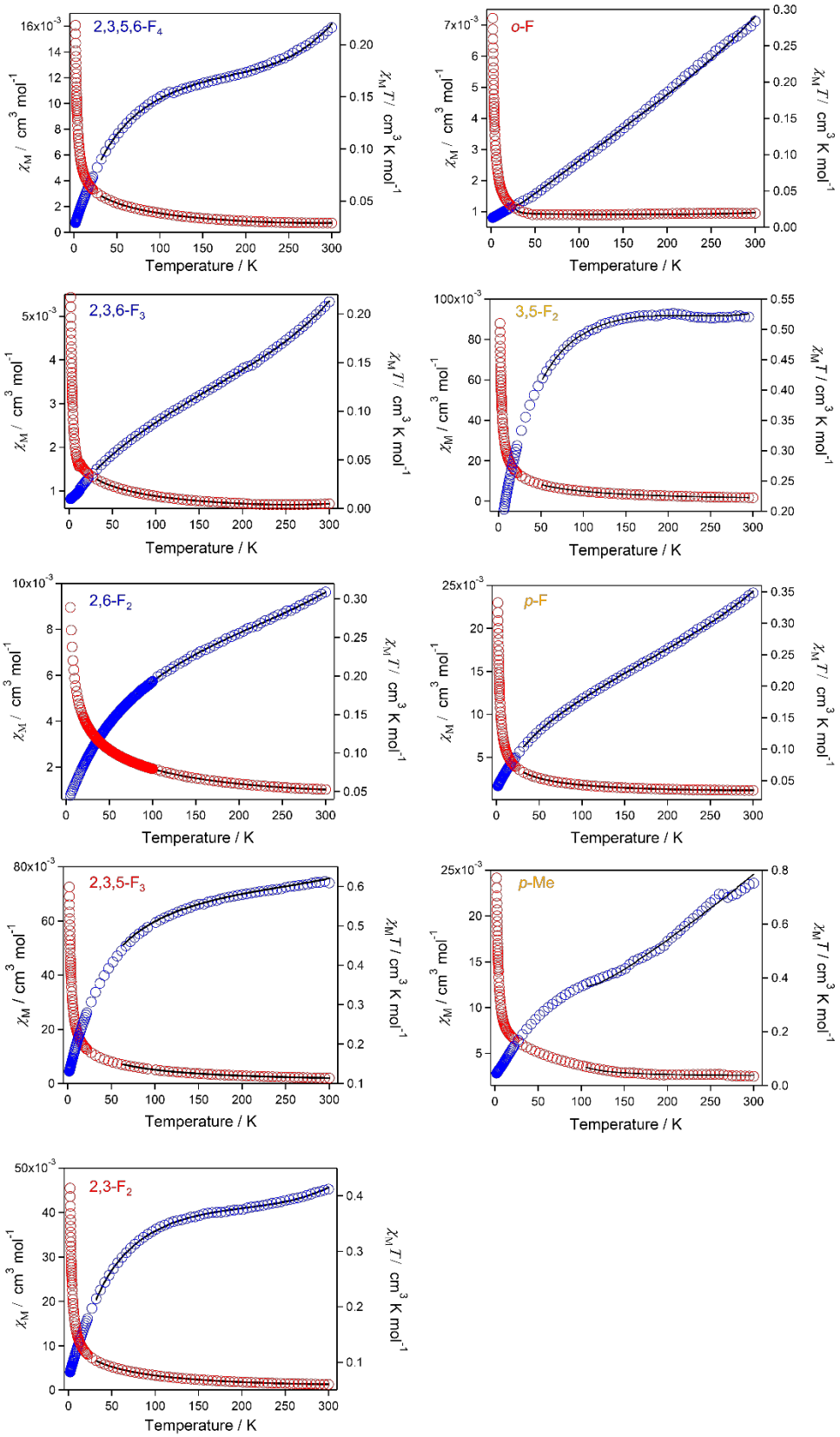

Figure S3. Plots of $\chi_M T$ vs. T for all complexes at 1.8−300 K under an external direct current field of 1 kOe. Solid lines show the best fits by assuming only singlet ground state and triplet excited state are populated with Boltzmann distribution with fitted parameters listed in Table S3.

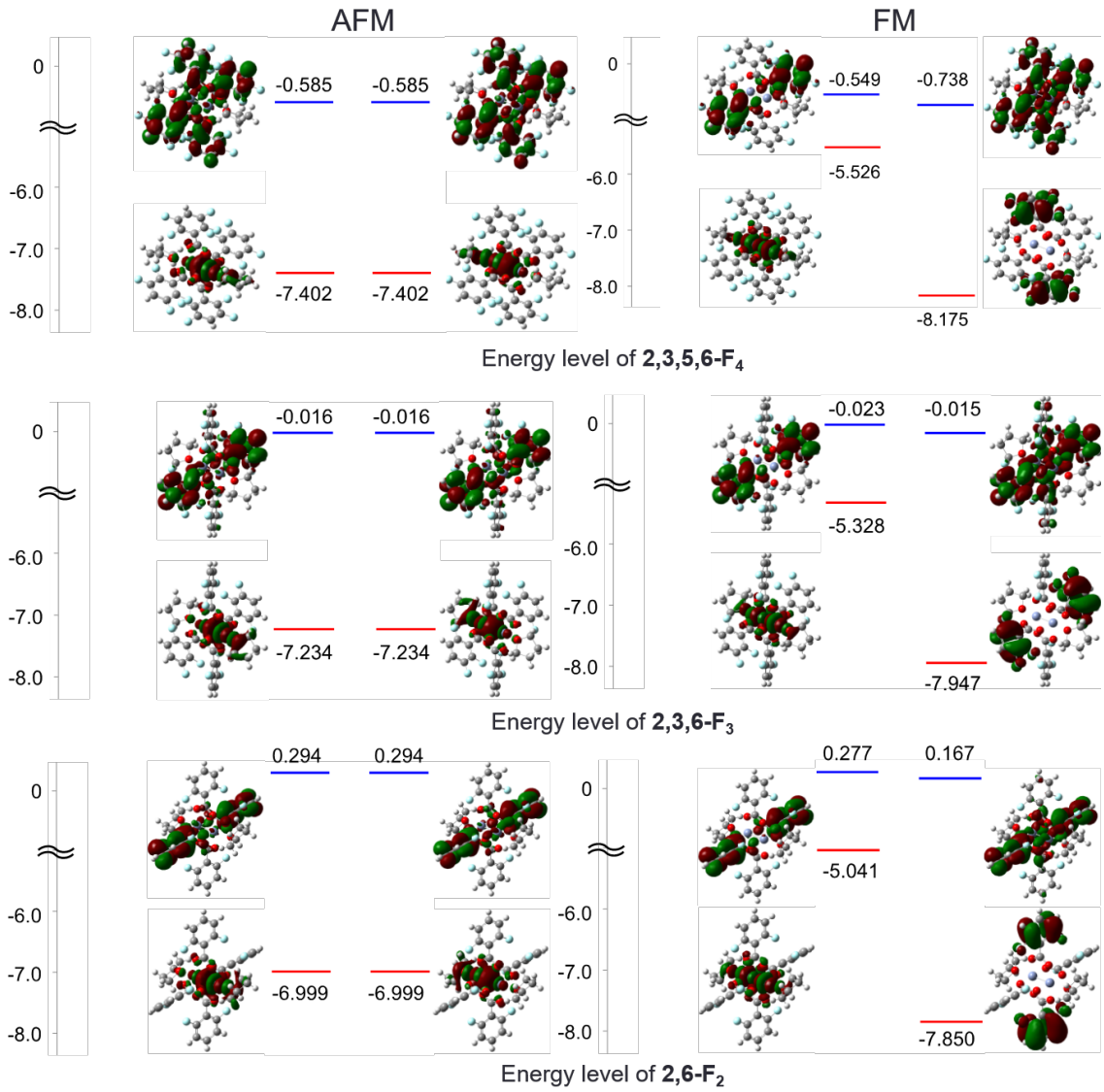

Figure S4. Energy level of frontier orbitals of [Cr_2] compounds with two *ortho*-F substitutions on benzoate bridges with HOMO and LUMO levels indicated by red and blue lines, respectively. The left and right lines correspond to α and β orbitals, respectively, while values under those lines are orbital energy values (in eV).

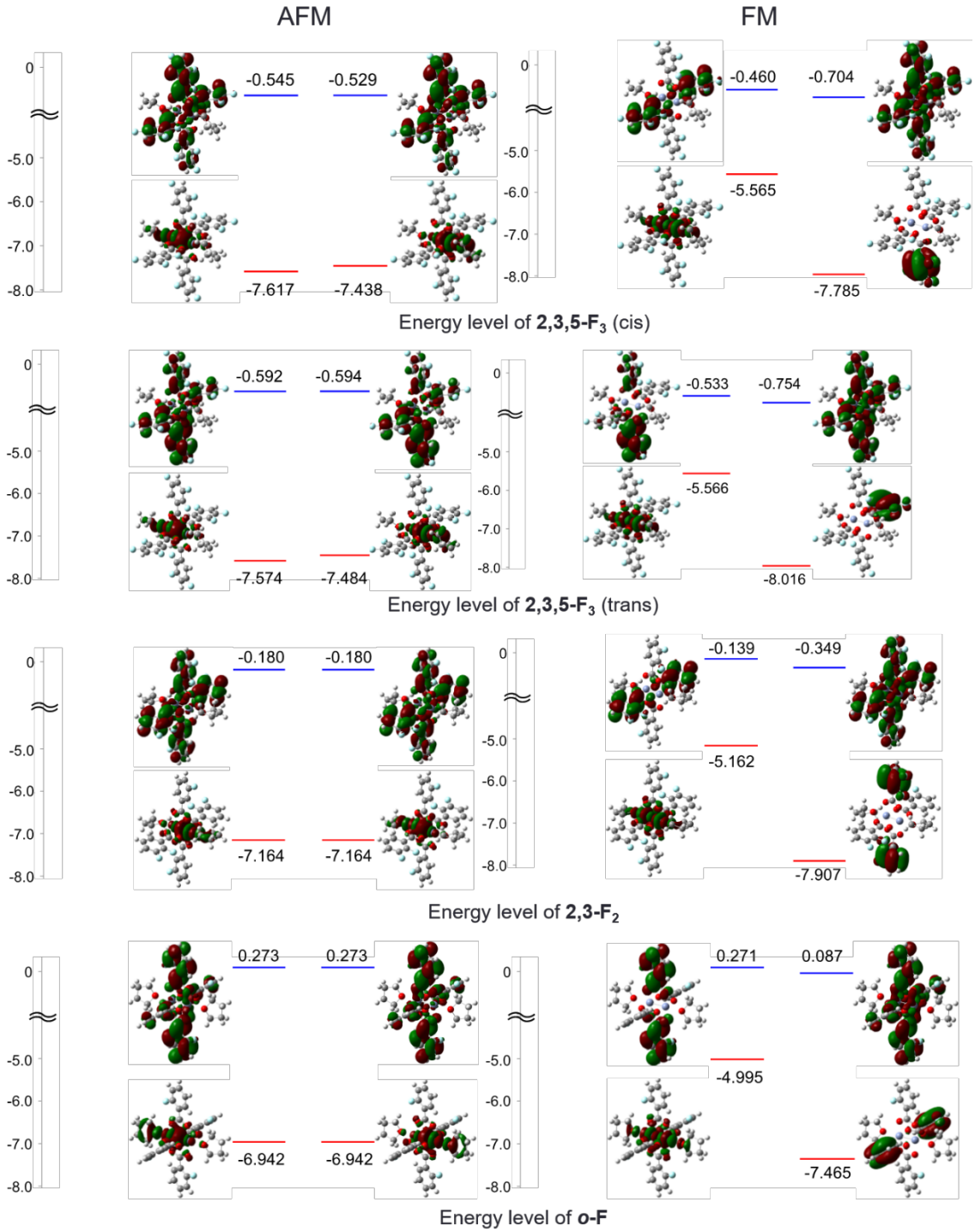

Figure S5. Energy level of frontier orbitals of [Cr_2] compounds with one *ortho*-F substitution on benzoate bridges with HOMO and LUMO levels indicated by red and blue lines, respectively. The left and right lines correspond to α and β orbitals, respectively, while values under those lines are orbital energy values (in eV).

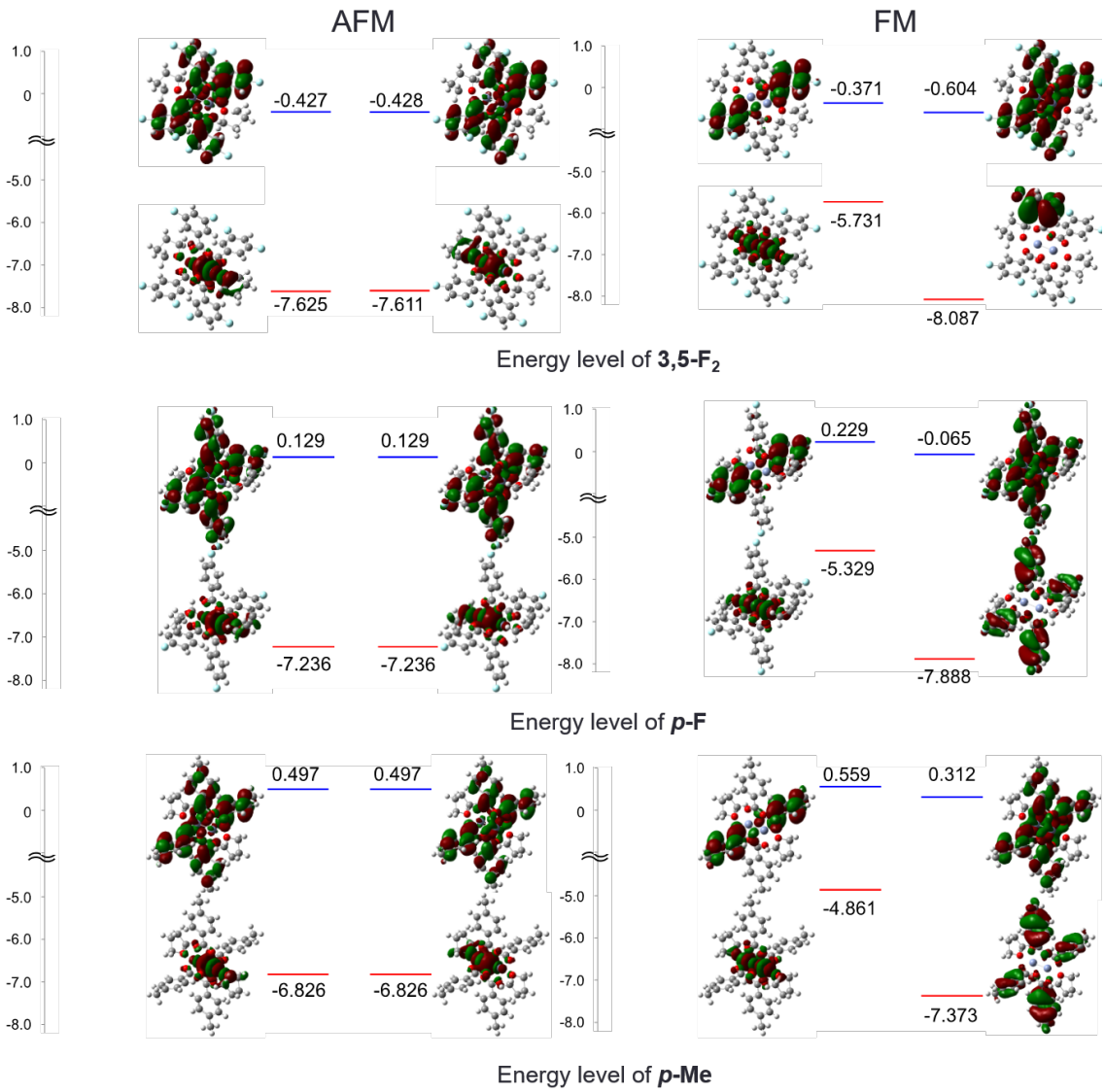

Figure S6. Energy level of frontier orbitals of [Cr_2] compounds with no *ortho*-F substitution on benzoate bridges with HOMO and LUMO levels indicated by red and blue lines, respectively. The left and right lines correspond to α and β orbitals, respectively, while values under those lines are orbital energy values (in eV).

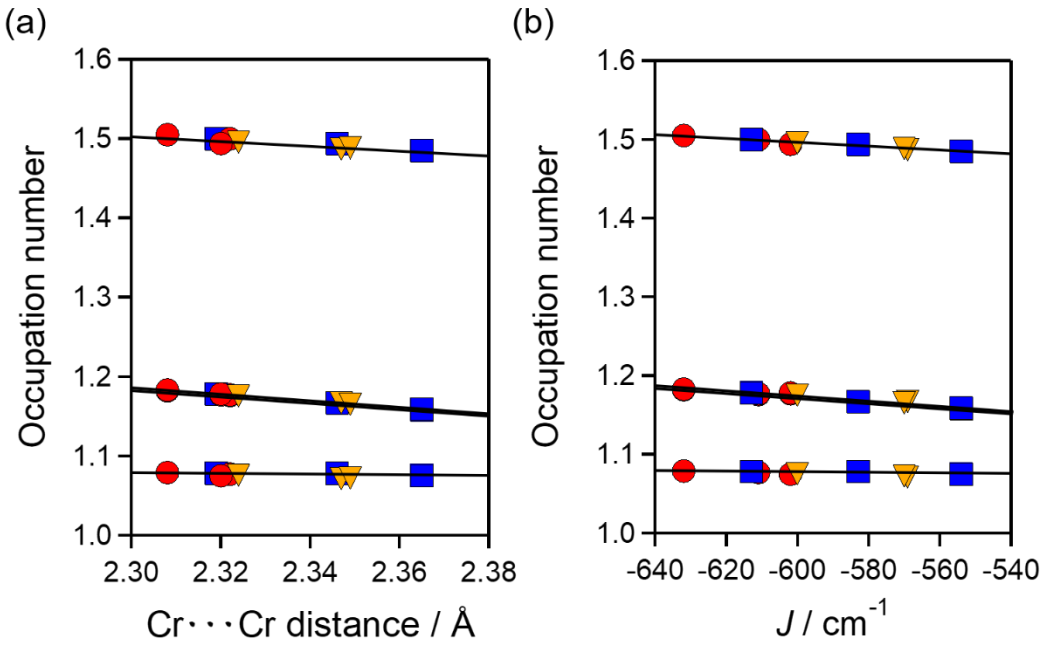

Figure S7. (a) Cr···Cr distance and (b) *J* dependence of occupation number of σ, π, and δ orbitals for each complex (the same categorization mentioned in the caption of Fig. S1). Black solid lines represent the best fits of data.

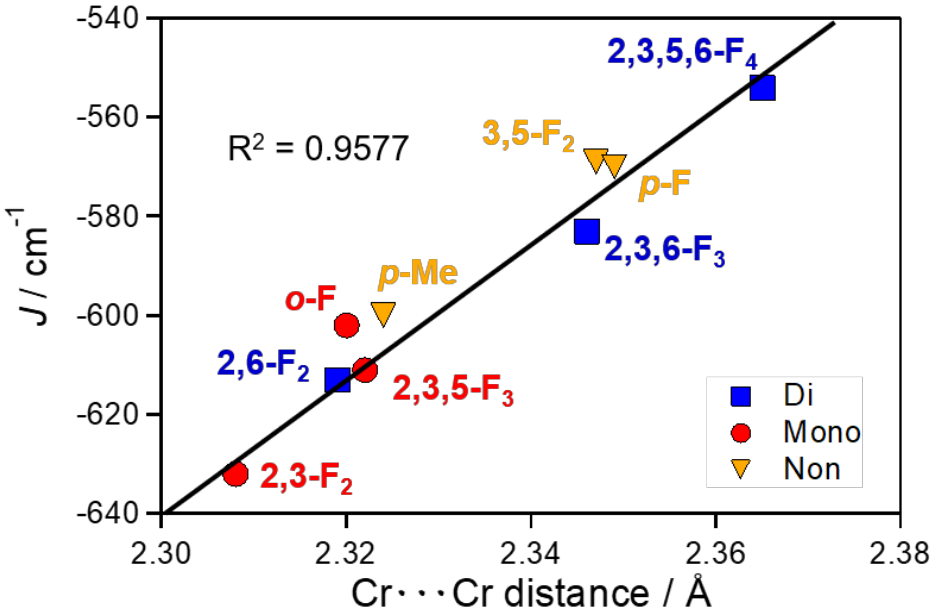

Figure S8. Plot of coupling constant *J* vs. Cr···Cr distance with same classification indicated in the caption of Fig. S1, while the solid line represents the best fit.

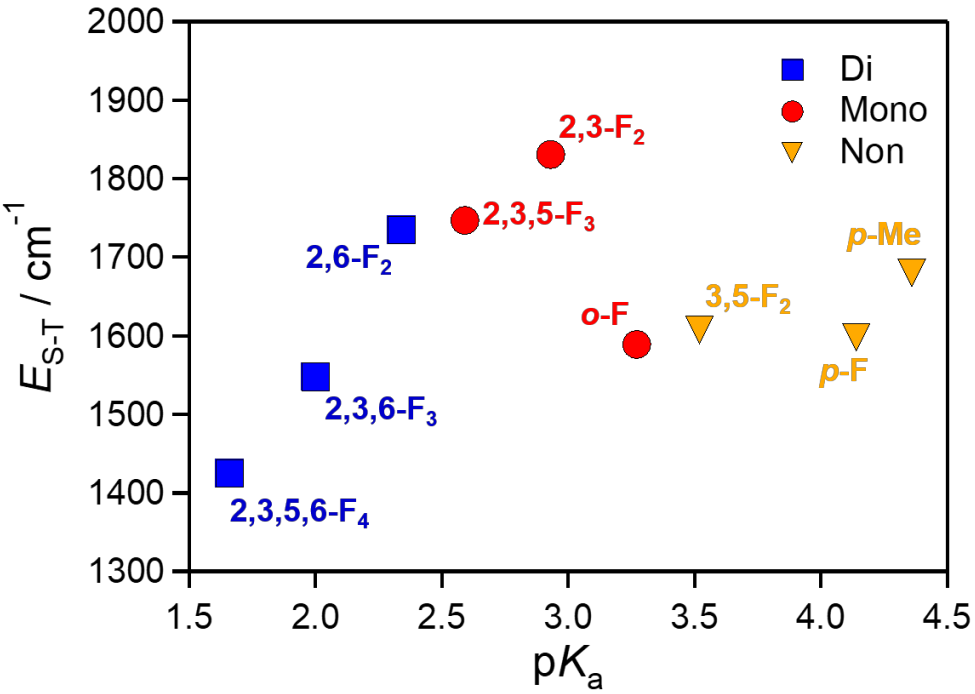

Figure S9. Benzoic-acid-pK_a-dependent Cr−Cr coupling constant for [Cr_2] complexes with same classification indicated in the caption of Fig. S1

Table S1. Crystallographic data for $[Cr_2(RCO_2)_4(THF)_2]$.

	2,3,5,6-F$_4$	**2,3,6-F$_3$**	**2,6-F$_2$**	**2,3,5-F$_3$**	**2,3-F$_2$**	***o*-F**	**3,5-F$_2$**	***p*-F**	***p*-Me**
Formula	$C_{36}H_{20}Cr_2F_{16}O_{10}$	$C_{36}H_{24}Cr_2F_{12}O_{10}$	$C_{36}H_{28}Cr_2F_8O_{10}$	$C_{40}H_{32}Cr_2F_{12}O_{11}$	$C_{36}H_{28}Cr_2F_8O_{10}$	$C_{36}H_{32}Cr_2F_4O_{10}$	$C_{36}H_{28}Cr_2F_8O_{10}$	$C_{36}H_{32}Cr_2F_2O_{10}$	$C_{46}H_{58}Cr_2F_2O_{10}$
Formula weight	1020.51	948.55	876.59	1020.66	876.59	804.63	876.59	804.63	875.95
Crystal system	Monoclinic	Monoclinic	Monoclinic	Monoclinic	Triclinic	Monoclinic	Monoclinic	Monoclinic	Triclinic
Space group	$P2_1/c$	$P2_1/c$	$P2_1/c$	Cc	$P\bar{1}$	$C2/c$	$P2_1/n$	$P2_1/c$	$P\bar{1}$
a (Å)	8.822(3)	9.6371(12)	9.429(6)	14.874(3)	7.7406(17)	19.18(2)	10.718(9)	9.1220(14)	9.0987(12)
b (Å)	16.921(6)	11.3166(13)	11.203(7)	15.244(3)	10.942(3)	9.262(8)	10.847(8)	17.927(3)	10.5190(16)
c (Å)	13.021(5)	16.746(2)	17198(11)	18.470(4)	10.945(3)	21.08(2)	16.129(12)	11.1326(17)	12.2273(19)
α (°)	90	90	90	90	106.608(5)	90	90	90	81.196(6)
β (°)	109.560(5)	100.3523(13)	101.896(10)	95.212(4)	92.5406(11)	111.820(12)	94.519(14)	109.3342(19)	74.405(6)
γ (°)	90	90	90	90	100.923(4)	90	90	90	73.368(5)
V (Å^3)	1831.7(12)	1796.6(4)	1778(2)	4170.4(16)	847.4(4)	3477(6)	1869(3)	1717.9(4)	1076.3(3)
Z	2	2	2	4	1	4	2	2	2
T (K)	103	103	103	103	103	103	103	103	103
D_{calc} (g/cm^3)	1.850	1.753	1.638	1.625	1.678	1.537	1.557	1.555	1.350
μ (mm^{-1})	0.735	0.727	0.712	0.635	0.730	0.705	0.677	0.713	0.562
Unique reflns [R(int)]	1016 [0.0489]	952 [0.0167]	888 [0.0769]	2064 [0.0813]	444 [0.0126]	1648 [0.1164]	888 [0.0638]	824 [0.0200]	462 [0.0233]
R_1[a] wR_2[b] [$I>2\sigma(I)$]	0.0526 0.1032	0.0284 0.0756	0.0889 0.1749	0.0745 0.1943	0.0357 0.0857	0.0886 0.2145	0.0851 0.1839	0.0471 0.1196	0.0478 0.1195
R_1 wR_2 (all data)	0.0788 0.1156	0.0301 0.0767	0.1267 0.1966	0.0993 0.2251	0.0431 0.0920	0.1004 0.2360	0.1160 0.2035	0.0490 0.1215	0.0594 0.1275
CCDC	1876325	1876320	1876324	1876326	1876318	1876321	1876319	1876322	1876323

[a] $R_1 = (\Sigma \| F_o \| - \| F_c \|) / \Sigma | F_o |$, [b] $wR_2 = \{\Sigma [w(F_o^2 - F_c^2)^2] / \Sigma [w(F_o^2)]^2\}^{1/2}$

Table S2. Selected bond lengths and angles for $[Cr_2(RCO_2)_4(THF)_2]$.

	2,3,5,6-F_4	**2,3,6-F_3**	**2,6-F_2**
Cr(1)−Cr(1)#1	2.3655(10)	2.3460(5)	2.3192(17)
Cr(1)−O(1)	2.0154(17)	2.0034(10)	2.011(3)
Cr(1)−O(2)#1	2.0141(17)	2.0244(10)	2.030(3)
Cr(1)−O(3)	2.0214(18)	2.0182(10)	2.022(3)
Cr(1)−O(4)#1	2.0165(18)	2.0145(10)	2.024(3)
Cr(1)−O(5)	2.2284(18)	2.2330(10)	2.239(3)
Cr(1)#1−Cr(1)−O(1)	86.27(5)	87.25(3)	88.28(9)
Cr(1)#1−Cr(1)−O(2)#1	90.24(5)	89.67(3)	89.5(1)
Cr(1)#1−Cr(1)−O(3)	89.06(5)	88.08(3)	89.73(9)
Cr(1)#1−Cr(1)−O(4)#1	87.45(5)	88.90(3)	88.15(9)
Cr(1)#1−Cr(1)−O(5)	173.87(6)	173.73(3)	175.09(7)
O(1)−Cr(1)−O(2)#1	176.40(6)	176.92(4)	177.78(11)
O(1)−Cr(1)−O(3)	91.92(8)	89.61(4)	90.15(11)
O(1)−Cr(1)−O(4)#1	89.95(8)	90.39(4)	89.32(11)
O(1)−Cr(1)−O(5)	87.74(7)	86.55(4)	86.83(11)
O(2)#1−Cr(1)−O(3)	87.09(8)	90.28(4)	89.42(11)
O(2)#1−Cr(1)−O(4)#1	90.82(8)	89.55(4)	91.03(11)
O(2)#1−Cr(1)−O(5)	95.72(7)	96.54(4)	95.36(11)
O(3)−Cr(1)−O(4)#1	175.92(6)	176.98(4)	177.83(11)
O(3)−Cr(1)−O(5)	89.82(7)	90.96(4)	90.71(11)
O(4)#1−Cr(1)−O(5)	93.88(7)	92.05(4)	91.37(11)
		Symmetry operation	
	#1 –x, –y+1, –z+1	#1 –x+2, –y+1, –z+1	#1 –x, –y+1, –z+1

		2,3,5-F_3	
Cr(1)−Cr(2)	2.3221(14)		
Cr(1)−O(2)	2.000(5)	Cr(2)−O(1)	2.012(5)
Cr(1)−O(4)	2.026(5)	Cr(2)−O(3)	2.009(5)
Cr(1)−O(6)	2.017(5)	Cr(2)−O(5)	2.018(5)
Cr(1)−O(8)	2.029(5)	Cr(2)−O(7)	2.017(5)
Cr(1)−O(10)	2.251(5)	Cr(2)−O(9)	2.252(5)
Cr(2)−Cr(1)−O(2)	88.64(15)	Cr(1)−Cr(2)−O(1)	88.8(1)
Cr(2)−Cr(1)−O(4)	89.78(15)	Cr(1)−Cr(2)−O(3)	88.1(1)
Cr(2)−Cr(1)−O(6)	89.07(15)	Cr(1)−Cr(2)−O(5)	88.6(2)
Cr(2)−Cr(1)−O(8)	87.07(15)	Cr(1)−Cr(2)−O(7)	90.4(2)
Cr(2)−Cr(1)−O(10)	174.06(16)	Cr(1)−Cr(2)−O(9)	173.8(2)
O(2)−Cr(1)−O(4)	90.0(2)	O(1)−Cr(2)−O(3)	90.6(2)
O(2)−Cr(1)−O(6)	177.5(2)	O(1)−Cr(2)−O(5)	177.3(2)
O(2)−Cr(1)−O(8)	90.8(2)	O(1)−Cr(2)−O(7)	89.6(2)
O(2)−Cr(1)−O(10)	93.5(2)	O(1)−Cr(2)−O(9)	90.9(2)
O(4)−Cr(1)−O(6)	89.1(2)	O(3)−Cr(2)−O(5)	90.0(2)
O(4)−Cr(1)−O(8)	176.7(2)	O(3)−Cr(2)−O(7)	178.5(2)
O(4)−Cr(1)−O(10)	95.8(2)	O(3)−Cr(2)−O(9)	85.7(2)
O(6)−Cr(1)−O(8)	90.0(2)	O(5)−Cr(2)−O(7)	89.7(2)
O(6)−Cr(1)−O(10)	88.9(2)	O(5)−Cr(2)−O(9)	91.9(2)
O(8)−Cr(1)−O(10)	87.4(2)	O(7)−Cr(2)−O(9)	95.8(2)

	2,3-F_2	***o*-F**	**3,5-F_2**
Cr(1)−Cr(1)#1	2.3079(6)	2.3208(19)	2.347(2)
Cr(1)−O(1)	2.0102(12)	2.025(3)	2.023(4)
Cr(1)−O(2)#1	2.0082(12)	2.020(3)	2.028(4)
Cr(1)−O(3)	2.0157(12)	2.027(3)	2.031(4)
Cr(1)−O(4)#1	2.0084(12)	2.020(3)	2.054(4)
Cr(1)−O(5)	2.2512(12)	2.275(3)	2.264(5)
Cr(1)#1−Cr(1)−O(1)	88.03(4)	89.68(11)	89.58(12)
Cr(1)#1−Cr(1)−O(2)#1	89.88(4)	88.41(11)	87.66(12)
Cr(1)#1−Cr(1)−O(3)	89.43(4)	89.45(9)	88.95(12)
Cr(1)#1−Cr(1)−O(4)#1	88.44(4)	88.20(9)	88.21(12)
Cr(1)#1−Cr(1)−O(5)	174.94(4)	173.25(8)	176.38(13)
O(1)−Cr(1)−O(2)#1	177.90(5)	177.82(10)	177.23(16)
O(1)−Cr(1)−O(3)	91.11(5)	88.58(12)	90.29(15)
O(1)−Cr(1)−O(4)#1	89.57(5)	91.58(13)	88.38(15)
O(1)−Cr(1)−O(5)	90.98(5)	95.86(12)	93.63(16)
O(2)#1−Cr(1)−O(3)	89.06(5)	90.35(13)	89.85(15)
O(2)#1−Cr(1)−O(4)#1	90.18(5)	89.41(13)	91.34(15)
O(2)#1−Cr(1)−O(5)	91.09(5)	86.12(12)	89.12(17)
O(3)−Cr(1)−O(4)#1	177.74(5)	177.64(10)	176.87(17)
O(3)−Cr(1)−O(5)	95.55(5)	94.54(11)	92.70(16)
O(4)#1−Cr(1)−O(5)	86.59(5)	87.79(12)	90.21(16)
		Symmetry operation	
	#1 –x+1, –y+2, –z+1	#1 –x+2, –y+1, –z+1	#1 –x, –y, –z+1

	***p*-F**	***p*-Me**
Cr(1)−Cr(1)#1	2.3490(6)	2.3242(8)
Cr(1)−O(1)	2.0123(15)	2.0110(16)
Cr(1)−O(2)#1	2.0135(15)	2.0091(17)
Cr(1)−O(3)	2.0045(16)	2.0052(16)
Cr(1)−O(4)#1	2.0190(16)	2.0148(16)
Cr(1)−O(5)	2.2954(14)	2.3018(17)
Cr(1)#1−Cr(1)−O(1)	89.47(4)	87.31(5)
Cr(1)#1−Cr(1)−O(2)#1	87.45(4)	90.15(4)
Cr(1)#1−Cr(1)−O(3)	89.14(4)	89.01(5)
Cr(1)#1−Cr(1)−O(4)#1	87.76(4)	88.45(5)
Cr(1)#1−Cr(1)−O(5)	174.55(5)	174.21(5)
O(1)−Cr(1)−O(2)#1	176.83(5)	177.30(6)
O(1)−Cr(1)−O(3)	89.11(7)	90.17(7)
O(1)−Cr(1)−O(4)#1	88.99(6)	91.91(7)
O(1)−Cr(1)−O(5)	93.79(6)	88.11(6)
O(2)#1−Cr(1)−O(3)	90.11(7)	88.86(7)
O(2)#1−Cr(1)−O(4)#1	91.62(6)	88.94(7)
O(2)#1−Cr(1)−O(5)	89.34(6)	94.48(6)
O(3)−Cr(1)−O(4)#1	176.39(6)	176.63(7)
O(3)−Cr(1)−O(5)	95.26(6)	94.55(7)
O(4)#1−Cr(1)−O(5)	87.93(6)	88.16(7)

Symmetry operation

#1 –x+1, –y+1, –z #1 –x+2, –y+2, –z

Table S3. Fitted parameters (fixed $g = 2$) extracted from magnetic data of $[Cr_2(RCO_2)_4(THF)_2]$ compared with J and $R_{Cr\cdots Cr}$ values.

Complex	TIP/10^{-5} cm^3 mol^{-1}	$P/10^{-4}$	θ/K	E_{S-T}/cm^{-1}	J /cm^{-1}	$R_{Cr\cdots Cr}$/Å
2,3,5,6-F$_4$	3.6(1)	3.68(5)	−45(1)	1425(11)	−554	2.365
2,3,6-F$_3$	46.1(3)	1.01(2)	−43(1)	1548(6)	−583	2.346
2,6-F$_2$	30.6(7)	4.04(4)	−49(1)	1735(25)	−613	2.319
2,3,5-F$_3$	6.2(2)	108(1)	−29(1)	1747(11)	−611	2.322
2,3-F$_2$	41.1(3)	7.20(1)	−32(1)	1831(18)	−632	2.308
***o*-F**	90.7(5)	0.115(3)	−24(1)	1589(39)	−602	2.320
3,5-F$_2$	40.6(2)	11.5(9)	−30.2(5)	1607(11)	−569	2.347
***p*-F**	71.0(4)	21.4(1)	−18.4(3)	1598(12)	−570	2.349
***p*-Me**	57.0(9)	5.70(9)	−73(5)	1680(12)	−600	2.324

Table S4. Energy of HS and LS states, coupling constant J, and $R_{Cr\cdots Cr}$ of $[Cr_2(RCO_2)_4(THF)_2]$.

Complex	Ferromagnetic (HS)		Antiferromagnetic (LS)		J /cm^{-1}	$R_{Cr\cdots Cr}$/Å
	E / a.u.	$<S^2>$	E / a.u.	$<S^2>$		
2,3,5,6-F$_4$	−5820.498393	20.0119	−5820.539481	3.7224	−554	2.36540
2,3,6-F$_3$	−5423.680310	20.0118	−5423.723589	3.7075	−583	2.34581
2,6-F$_2$	−5026.847143	20.0125	−5026.892716	3.6936	−613	2.31912
2,3,5-F$_3$ (cis)	−5423.673545	20.0127	−5423.718951	3.6944	−611	2.32198
2,3,5-F$_3$ (trans)	−5423.679130	20.0128	−5423.724548	3.6948	−611	2.32198
2,3-F$_2$	−5026.843188	20.0129	−5026.890198	3.6850	−632	2.30802
***o*-F**	−4630.028457	20.0122	−4630.073239	3.7003	−602	2.32024
3,5-F$_2$	−5026.798302	20.0121	−5026.840584	3.7154	−569	2.34701
***p*-F**	−4630.033363	20.0123	−4630.075670	3.7156	−570	2.34891
***p*-Me**	−4390.281464	20.0129	−4390.326070	3.7013	−600	2.32422

Table S5. Energy level of frontier orbitals in AFM state for $[Cr_2(RCO_2)_4(THF)_2]$.

Complex	Alpha / eV				Beta / eV			
	HOMO	π		LUMO	HOMO	π		LUMO
2,3,5,6-F$_4$	−7.4018	−8.3392	−8.5202	−0.5856	−7.4017	−8.3392	−8.5212	−0.5849
2,3,6-F$_3$	−7.2343	−8.2380	−8.4045	−0.0166	−7.2343	−8.2385	−8.4040	−0.0167
2,6-F$_2$	−6.9993	−7.9438	−7.9727	0.2938	−6.9994	−7.9441	−7.9727	0.2938
2,3,5-F$_3$ (cis)	−7.6170	−8.5555	−8.7115	−0.5455	−7.4385	−8.4200	−8.5977	−0.5287
2,3,5-F$_3$ (trans)	−7.5738	−8.4804	−8.6559	−0.5919	−7.4835	−8.4930	−8.6353	−0.5940
2,3-F$_2$	−7.1642	−8.1373	−8.2627	−0.1802	−7.1642	−8.1381	−8.2619	−0.1802
***o*-F**	−6.9421	−7.9631	−8.0407	0.2428	−6.9420	−7.9642	−8.0418	0.2427
3,5-F$_2$	−7.6249	−8.5153	−8.7468	−0.4268	−7.6116	−8.6421	−8.7346	−0.4282
***p*-F**	−7.2365	−8.1754	−8.2734	0.1291	−7.2365	−8.1751	−8.2736	0.1290
***p*-Me**	−6.8264	−7.7479	−7.8445	0.4969	−6.8264	−7.7479	−7.8448	0.4967